Acta Pharmaceutica Sinica B 2019;9(3):516–525

Chinese Pharmaceutical Association
Institute of Materia Medica, Chinese Academy of Medical Sciences

Acta Pharmaceutica Sinica B

www.elsevier.com/locate/apsb
www.sciencedirect.com

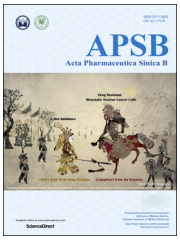

ORIGINAL ARTICLE

Secalonic acid D induces cell apoptosis in both sensitive and ABCG2-overexpressing multidrug resistant cancer cells through upregulating c-Jun expression

Hong Zhang[a], Liyan Huang[a], Liyang Tao[a], Jianye Zhang[b], Fang Wang[a], Xu Zhang[a], Liwu Fu[a,*]

[a]*Sun Yat-sen University Cancer Center, State Key Laboratory of Oncology in South China, Collaborative Innovation Center for Cancer Medicine, Guangdong Esophageal Cancer Institute, Guangzhou 510060, China*
[b]*School of Pharmaceutical Sciences, Guangzhou Medical University, Guangzhou 511436, China*

Received 30 September 2018; received in revised form 4 November 2018; accepted 28 November 2018

KEY WORDS

Multidrug resistance;
Secalonic acid D;
Apoptosis;
c-Jun;
ABCG2

Abstract Secalonic acid D (SAD) could inhibit cell growth in not only sensitive cells but also multidrug resistant (MDR) cells. However, the molecular mechanisms need to be elucidated. Here, we identified that SAD possessed potent cytotoxicity in 3 pairs of MDR and their parental sensitive cells including S1-MI-80 and S1, H460/MX20 and H460, MCF-7/ADR and MCF-7 cells. Furthermore, SAD induced cell G2/M phase arrest *via* the downregulation of cyclin B1 and the increase of CDC2 phosphorylation. Importantly, JNK pathway upregulated the expression of c-Jun in protein level and increased c-Jun phosphorylation induced by SAD, which was linked to cell apoptosis *via* c-Jun/Src/STAT3 pathway. To investigate the mechanisms of upregulation of c-Jun protein by SAD, the mRNA expression level and degradation of c-Jun were examined. We found that SAD did not alter the mRNA level of c-Jun but inhibited its proteasome-dependent degradation. Taken together, these results implicate that SAD induces cancer cell death through c-Jun/Src/STAT3 signaling axis by inhibiting the proteasome-dependent degradation of c-Jun in both sensitive cells and ATP-binding cassette transporter sub-family G member 2 (ABCG2)-mediated MDR cells.

Abbreviations: ABCB1, ATP-binding cassette subfamily B member 1; ABCG2, ATP-binding cassette transporter sub-family G member 2; AP-1, activating protein-1; CHX, cycloheximide; HUVEC, human umbilical vein endothelial cells; JNKs, c-Jun N-terminal kinases; MAPKs, mitogen-activated protein kinases; MDR, multidrug resistance; MTT, 3-(4,5-dimethylthiazol-yl)-2,5-diphenyltetrazolium bromide; NCM460, human normal colon epithelial cells; RT-PCR, Real-time polymerase chain reaction; SAD, Secalonic acid D; SDS-PAGE, sodium dodecyl sulfate-polyacrylamide gel electrophoresis; SP, side population

*Corresponding author. Tel.: +86 20 87343163; fax: +86 20 87343170.
E-mail address: Fulw@mail.sysu.edu.cn (Liwu Fu).

Peer review under responsibility of Institute of Materia Medica, Chinese Academy of Medical Sciences and Chinese Pharmaceutical Association.

https://doi.org/10.1016/j.apsb.2018.12.006

1. Introduction

The marine organisms account for 78% of the total biomasses[1,2]. Marine species induce and accumulate amounts of compounds with special construction and physiology activity in this broad and unique environment. Due to the unique genetic background and metabolic pathways, mangrove endophytic fungi present a complicated structure and a variety of biological activity for its metabolites[3]. Secalonic acid D (SAD) was a marine compound separated from the secondary metabolite of the mangrove endophytic fungus[4]. Our prior research demonstrated that SAD induced leukemia cell apoptosis *via* GSK-3*β*/*β*-catenin/c-Myc pathway[5]. Furthermore, we also found that SAD exerted antitumor effect on MDR cells through decreasing the expression of ABCG2[6]. However, the molecular mechanisms by which SAD overcomes MDR remain unclear.

Protein kinase and phosphatase signaling networks, like mitogen-activated protein kinases (MAPKs), may be considered as new targets for cancer therapy through regulating cell growth, apoptosis, and differentiation[7]. c-Jun N-terminal kinases (JNKs) are a set of MAPKs in response to various environmental stresses and cytokines. Several studies reported that JNKs regulate the expression of MDR-associated *ABCG2* and ATP-binding cassette subfamily B member 1 (*ABCB1*) genes[8,9]. Hence, we speculated that SAD might affect JNK signaling pathway in MDR cells. The JNKs were shown to specifically bind to the N-terminal sites of c-Jun, an essential component of activating protein-1 (AP-1), which was located on 1p32-p31 involved in a high frequency of translocations and deletions in human cancers[10]. It was reported that JNKs promoted the activity of c-Jun by phosphorylating it at serines 63 and 73[11]. c-Jun was primarily reported as a proto-oncoprotein that regulates cell proliferation, apoptosis, and metastasis. However, it may also exert anti-oncogene effects in cancer. Karoline et al.[12] showed that c-Jun prevented the silence of p16INK4a by depressing its methylation, which resulted in tumor suppression and cell cycle arrest. Meanwhile, the overexpression of c-Jun could induce apoptosis in B cell leukemia[13].

In this study, we found that SAD triggered the apoptosis of cancer cells through JNK/c-Jun signaling pathway. Upregulating or down-regulating c-Jun expression could promote or suppress apoptosis in both MDR cells and their parental cells. Importantly, SAD enhanced the JNK-dependent phosphorylation of c-Jun and increased the level of c-Jun in the cell nucleus. Meanwhile, we observed that the c-Jun protein was stabilized by SAD treatment which decreased its proteasomal-mediated degradation. In addition, our results further presented that the overexpression of c-Jun facilitated apoptosis through inhibiting Src/STAT3 signaling in MDR cells.

2. Materials and methods

2.1. Chemicals and reagents

SAD with a purity of >98% were isolated from metabolites of marine-derived mangrove endophytic fungus and dissolved in DMSO for use at indicated concentrations. GAPDH antibody was purchased from Kangchen Co. (Shanghai, China). Antibodies against c-Jun (9165), p-c-Jun (2361), JNK (9258), p-JNK (9251), HistoneH3 (11885), Src (2109), p-Src (2101), STAT3 (9139), p-STAT3 (9131) were purchased from Cell Signaling Technology (Boston, Massachusetts, USA). Cyclin B1, CDC2 and p-CDC2 (Tyr15) were purchased from Affinity Biosciences (USA). RT Kit was from Thermo Fisher Scientific Inc. (Waltham, MA, USA). MG132, 3-(4,5-dimethylthiazol-yl)-2,5-diphenyltetrazolium bromide (MTT) and other chemicals were purchased from Sigma Chemical Co. (Shanghai, China).

2.2. Cell lines and cell culture

The human colon carcinoma cell line S1, non-small cell lung cancer cell line H460, breast cancer line MCF-7 and their corresponding mitoxantrone-selected derivative ABCG2-overexpressing cell lines S1-MI-80, H460/MX20, and breast cancer line MCF-7, doxorubicin selected cell line MCF-7/ADR, as well as human normal colon epithelial cells (NCM460) and human umbilical vein endothelial cells (HUVEC) were cultured in DMEM containing 10% fetal bovine serum, 100 U/mL streptomycin and 100 U/mL penicillin at 37 °C in 5% (*v*/*v*) CO_2.

2.3. Cell cytotoxicity test

The MTT assay was used as previously described to examine cytotoxicity[13]. Briefly, cells were incubated in 96-well plates at the appropriate density and allowed to attach overnight. Then different concentrations of SAD were added to the wells. After 72 h, MTT (5 mg/mL, 20 μL/well) was added to each well for an additional 4 h. Subsequently, the medium was removed, and DMSO (100 μL/well) was added to dissolve purple MTT-formazan crystals. Finally, absorbance was measured at 540 nm with 630 nm as a reference filter by Model 550 Microplate Reader (Bio-Rad, Hercules, CA, USA). Experiments were performed triplicate. The concentration required to inhibit cell growth by 50% (IC_{50}) was calculated from survival curves using the Bliss method as previously reported[14].

2.4. Western blot analysis

After indicated treatment as showed in the figures, different cells were harvested and washed twice with ice-cold PBS buffer. Then cell extracts were collected with cell lysis buffer (1 × PBS, 0.1% SDS, 1% Nonidet P-40, 0.5% sodium deoxycholate, 100 mg/mL phenylmethylsulfonyl fluoride, 10 mg/mL leupeptin, 10 mg/mL aprotinin). Equal amounts of lysate protein from various treatments were resolved on sodium dodecyl sulfate-polyacrylamide gel electrophoresis (SDS-PAGE) gel and transferred to PVDF membrane (Pall, USA). After blocking with 5% fat-free milk, membranes were sequentially incubated with the primary and secondary antibodies. After washing three times with TBST buffer, the protein bands were visualized by the enhanced

Phototope TM-HRP Detection Kit (Cell Signaling, USA) and at last exposed to Kodak medical X-ray processor (Carestream Health, USA).

2.5. Cell cycle analysis

After S1 and S1-MI-80 cells were treated with the indicated concentrations, the cells were collected and washed twice with cold PBS. Then cells were fixed in 70% ice-cold ethanol overnight. After washing twice with PBS, 5×10^5 cells were resuspended in 0.5 mL PBS containing RNase A (100 μg/mL) and PI (100 μg/mL) for 30 min at 37 °C in the dark. The DNA content of cells was then analyzed by flow cytometer (Becton Dickinson, USA).

2.6. Cell apoptosis analysis

After SAD treatments, S1 and S1-MI-80 cells were stained with annexin V and propidium iodide (PI) (BD Pharmingen) and assessed by using flow cytometry. After treated with SAD or transfected with c-Jun shRNA or scramble vector, cells were digested with trypsin (EDTA-free) from EDTA and washed twice in ice-cold phosphate-buffered saline (PBS). A total of 5×10^5 cells were resuspended in 500 μL binding buffer, then 5 μL annexin V and 5 μL PI were added. After 15 min of incubation in the dark, cells were detected by flow cytometry. The apoptosis rate was calculated using Eq. (1):

$$\text{The apoptosis rate (\%)} = (\text{apoptotic cell population} / \text{total cell population observed}) \times 100 \quad (1)$$

2.7. Transfection of shRNA and plasmid DNA

The short hairpin RNA (shRNA) of c-Jun and its negative control were described as follow, the shRNA sequences of c-Jun were as follows: c-Jun shRNA (target sequence: 5′-GCAGCAG-CAGCCGCCGCACCA-3′) and control shRNA (target sequence: 5′-CAACAAGATGAAGAGCACCAA-3′). Cells were cultured in a 6-well plate in a density of 3×10^5 cells/well under media conditions. Then the cells were transfected with c-Jun shRNA or plasmid DNA in lipofectamine 2000 according to the manufacturer's instructions, the final concentration of c-Jun shRNA and the c-Jun plasmid was 4 μg/well. Cells were also transfected with lipofectamine 2000 containing control shRNA or scramble vector as a negative control. c-Jun shRNA and control shRNA lentiviral particles used to transfect S1 and S1-MI-80 cells were collected from viral packaging 293 T cells. The positive cells, transfected with c-Jun shRNA lentivirus, were sorted after puromycin (10 μg/mL) treatment.

2.8. Immunofluorescence analysis

Cells were collected and washed using PBS for twice, then fixed in 4% paraformaldehyde for 10 min. The cells were subjected to permeabilization using 0.1% Triton X-100 in PBS for 10 min at room temperature. Then, the cells were incubated for 1 h in 2% bovine serum albumin in PBS before incubation with a rabbit polyclonal c-Jun primary antibody (H-79 ×; Santa Cruz Biotechnology) overnight at 4 °C. Next, cells were washed three times with PBS and incubated with a goat anti-rabbit fluorescein-conjugated secondary antibody (Millipore Merck Chemicon, Pittsburgh, PA) for 1 h. The cells were washed three times with PBS and stained with DAPI for 30 min. Finally, the cells were washed and stained with 4′,6-diamidino-2-phenylindole; coverslips were then mounted using VECTASHIELD. A Leica TCS SP5 confocal microscope system (Leica Microsystems GmbH, Wetzlar, Germany) was used to visualize the cells and obtain fluorescent images.

2.9. RNA extraction and reverse transcription-PCR

Total cellular RNA was isolated by Trizol Reagent (Invitrogen, China) according to manufacturer's instruction. The first strand cDNA was synthesized by Oligo dT primers. PCR primers were 5′-GTGACCGCGACTTTTCAAAGC-3′ (forward) and 5′-CGTT GCTGGACTGGATTATCAG-3′ (reverse) for c-Jun, and 5′-CTTT GGTATCGTGGAAGGA-3′ (forward) and 5′- CACCCTGTTG CTGTAGCC-3′ (reverse) for *GAPDH*, respectively. The PCR reactions were carried out at 94 °C for 2 min for initial denaturation, followed by 94 °C for 30 s, 58 °C for 30 s, and 72 °C for 1 min with the GeneAmp PCR system9700 (PE Applied Biosystems, USA). After 35 cycles of amplification, additional extensions were done at 72 °C for 10 min. Products were resolved and examined by 1.5% agarose gel electrophoresis. All procedures were carried out based on the instructions.

2.10. Real-time polymerase chain reaction (RT-PCR)

For first-strand cDNA synthesis, 5 μg of total RNA was reverse-transcripted by using GoScript™ Reverse Transcription Kit (Promega). SYBR Green PCR Master Mix (Promega) labeling was used for 2-step quantitative real-time polymerase chain reaction (qRT-PCR).

2.11. Statistical analysis

Results were presented as means ± SD. Statistical analysis was done by Student's *t*-test analysis. The significance was determined at $P < 0.05$. All experiments were repeated at least three times.

3. Results

3.1. SAD exerted potent cytotoxicity against sensitive and MDR cells

MTT assay was used to detect the antitumor activity of SAD (Fig. 1A). The IC_{50} of SAD was 6.8 ± 1.7 μmol/L for S1 cells, 6.4 ± 1.1 μmol/L for S1-MI-80 cells, 5.3 ± 0.9 μmol/L for H460 cells, 4.9 ± 0.7 μmol/L for H460/MX20 cells, 5.1 ± 0.8 μmol/L for MCF-7 cells, 4.9 ± 1.1 μmol/L for MCF-7/ADR cells. After 72 h SAD treatment, we found that the proliferation of S1 and S1-MI-80 cells was inhibited in a concentration-dependent manner, as well as H460 and H460/MX20, MCF-7 and MCF-7/ADR cells (Fig. 1B, C and D). Comparing to the sensitive cells, SAD executed similar inhibition effects on the proliferation of MDR cells. We also examined in normal cell. The IC_{50} of SAD was 20.9 ± 6.1 μmol/L for NCM460 (Fig. 1E), and 14.9 ± 4.5 μmol/L for HUVEC (Fig. 1F). The results suggest that SAD is cytotoxic to both sensitive and MDR cells and hypotoxic to normal cells.

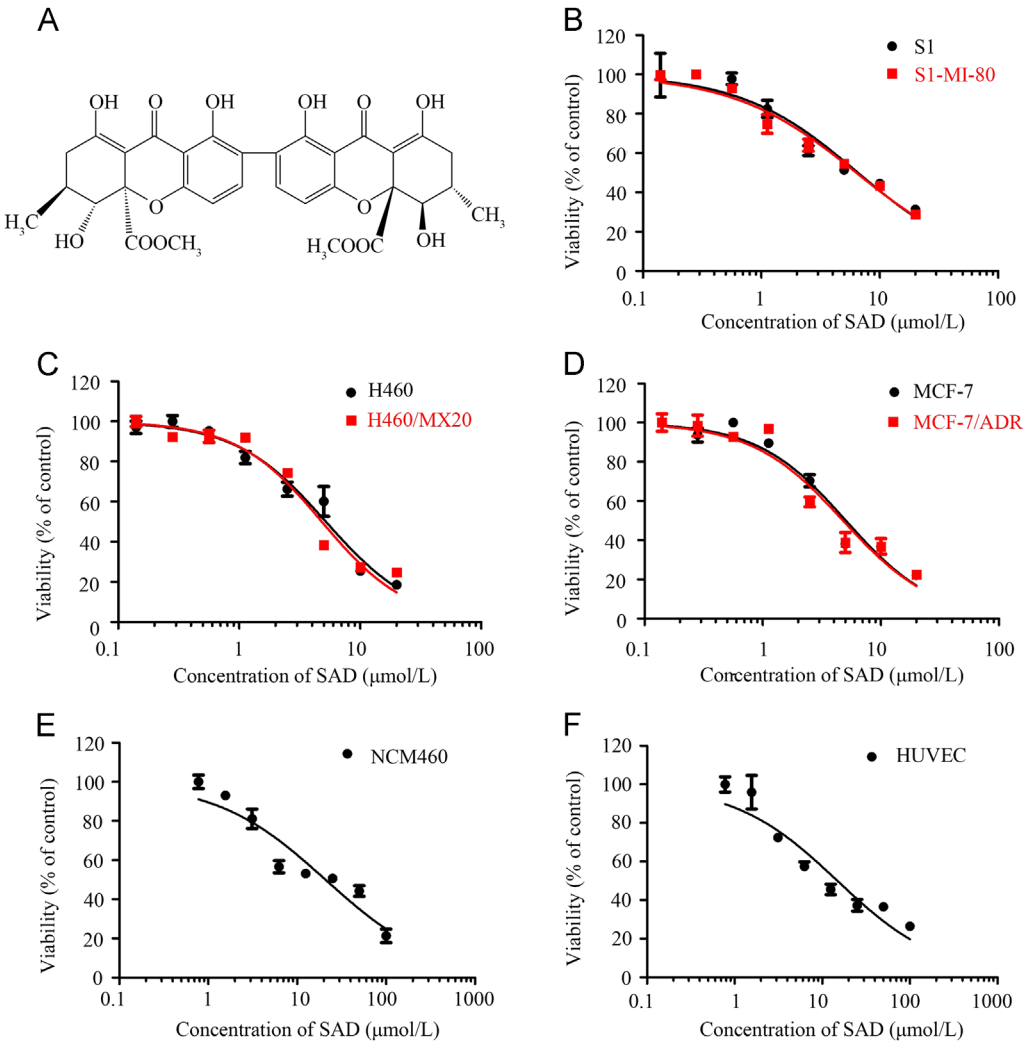

Figure 1 The structure and cytotoxic activity of secalonic acid D (SAD). (A) The chemical structure of SAD. (B)–(F) Cytotoxicity of SAD to S1 and S1-MI-80, H460 and H460/MX20, MCF-7 and MCF-7/ADR, NCM460 and HUVEC were determined by MTT assay as described in Methods. Each point represents the mean ± standard deviations (SD) of three independent experiments performed in triplicate.

3.2. *SAD induced G2/M phase arrest and apoptosis*

Previous study reported that SAD caused cell cycle arrest and programmed cell death in different kinds of human cells[5,15]. We detected the cell cycle of S1 and S1-MI-80 cells after SAD treatment by and flow cytometry analysis. The results showed that the treatment of SAD induced an increased number of cells in G2/M phase (Fig. 2A). After treating with 4 μmol/L SAD for 12, 24, 48, and 72 h, the content of G2/M phase was elevated from 12.0 ± 1.4% to 25.4 ± 5.0%, 30.1 ± 2.4%, 34.0 ± 2.8%, 44.7 ± 3.3% in S1 cells, and 13.5 ± 1.0% to 20.1 ± 1.8%, 26.8 ± 2.3%, 34.2 ± 2.0%, 36.4 ± 2.8% in S1-MI-80 cells, respectively (Fig. 2B). To further confirm the G2/M phase arrest induced by SAD, western blot analysis was used for detecting the expression of cyclin B1, p-CDC2, and CDC2. We found that the expression of cyclin B1 and CDC2 were significantly decreased in a time-dependent manner after SAD treatment, whereas the phosphorylation level of CDC2 was increased. As a result, the cyclin B1/CDC2 complex, a pivotal regulator of G2/M phase, was downregulated (Fig. 2C). To explore whether SAD could affect cancer cells apoptosis, annexin-V and PI double staining were used to distinguish apoptosis cells from the living cells. Then, the apoptotic rate of colon cancer cells S1 and S1-MI-80 was quantified by flow cytometry assay. After treating S1 cells and S1-MI-80 cells with 4 μmol/L SAD for 0, 24, 48 and 72 h, apoptotic rates were 2.3 ± 0.4%, 4.4 ± 1.2%, 10.7 ± 1.5%, and 20.9 ± 1.8% for S1 cells and 1.3 ± 0.1%, 6.8 ± 0.2%, 13.9 ± 2.6%, and 19.7 ± 0.3% for S1-MI-80 cells, respectively (Fig. 2D and E).

3.3. *SAD targeted JNK/c-Jun pathway*

It has been shown that JNK/c-Jun signaling pathway is related to MDR in colorectal cancer[16]. JNKs are a serine/threonine kinase superfamily which is efficiently regulated by a series of external stimuli and increases the activity of c-Jun[16]. In order to investigate the tumor-suppression mechanism of SAD, we studied whether SAD could activate JNK/c-Jun signaling. Western blot analysis showed that the total protein expression level and the phosphorylation level of both JNK and c-Jun significantly increased in a concentration-dependent manner after 48 h SAD treatment (Fig. 3A and B). These results

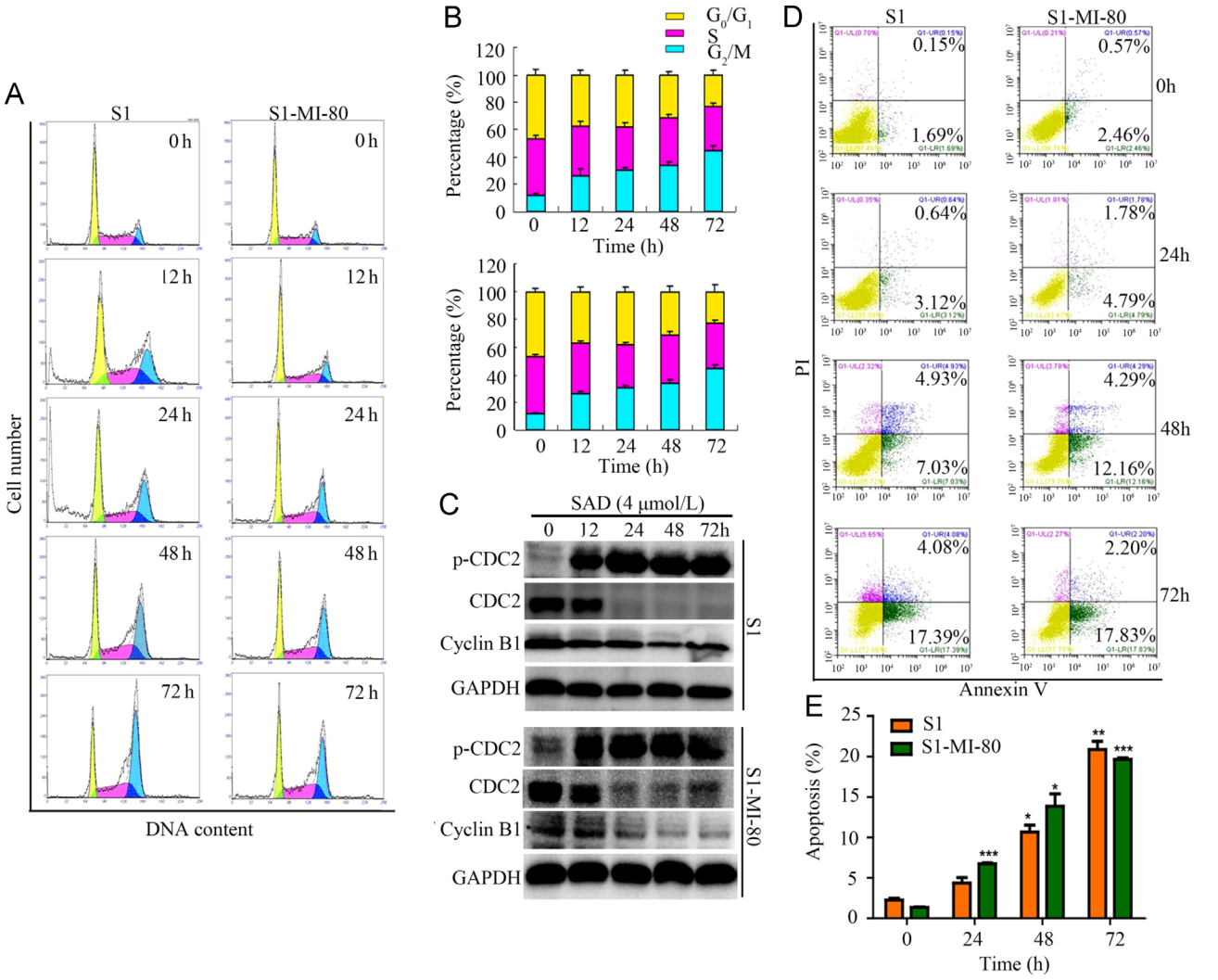

Figure 2 Effect of SAD on cell cycle and apoptosis. (A) The cell cycle analysis was determined by PI staining and flow cytometry cell quest software. S1 and S1-MI-80 cells were treated with 4 μmol/L SAD for 12, 24, 48, and 72 h, respectively. The content of G2/M phase was increased in a time-dependent pattern. (B) Histograms of cell cycle distribution in non-treated and treated S1 and S1-MI-80 cells. (C) S1 and S1-MI-80 cells were treated with SAD (4 μmol/L) for four different time points. Western blot analysis was used to detect the levels of CDC2, p-CDC2 and cyclin B1 protein after SAD treatment. (D) SAD-mediated cell apoptosis in S1 and S1-MI-80 cells were detected by flow cytometer. (E) Cells were incubated for 0, 24, 48 and 72 h in the presence or absence of SAD. The induction of cell apoptosis was detected by flow cytometry. $^{*}P < 0.05$, $^{**}P < 0.01$ and $^{***}P < 0.001$ *vs*. the control. Data were presented as mean ± SD from triplicate experiments.

indicate that JNK/c-Jun signaling is activated in SAD-treated S1 and S1-MI-80 cells.

3.4. *SAD treatment increased the nuclear level of c-Jun*

It was shown that c-Jun function as a transcription factor when it was transferred into the nucleus[15,17]. To study whether the nuclear level of c-Jun was increased, we used laser confocal microscopy to detect the location of c-Jun in S1 and S1-MI-80 cells. We found that after the treatment of SAD, c-Jun was upregulated compared with the negative control in the nucleus (Fig. 3C and D). Consistently with the discovery from immunofluorescence experiments, Western blot analysis also showed a time-dependent increase of nuclear c-Jun following SAD treatment (Fig. 3E). Meanwhile, the cytoplasmic level of c-Jun was also increased in a time-dependent manner (Fig. 3E).

3.5. *SAD promoted apoptosis through c-Jun increase*

To validate our hypothesis that SAD induces tumor cells death through c-Jun augmentation. S1 and S1-MI-80 cells were transiently transfected with 4 μg mock-vehicle, c-Jun plasmid or transfection reagents as vehicle control and treated with DMSO or SAD (4 μmol/L) over a 48-h time course. The protein level of c-Jun observed by Western blot was increased (Fig. 4A), and the apoptotic rate of cells was enhanced with c-Jun overexpression (Fig. 4B and D). Then, transfecting S1 and S1-MI-80 cells with a shRNA against c-Jun significantly downregulated the protein level of c-Jun (Fig. 4C). Flow cytometry assay showed that knocking down c-Jun could attenuate the effects of SAD on programmed cell death (Fig. 4B and D). These results indicate that the cytotoxic effect of SAD relates to the increase of c-Jun.

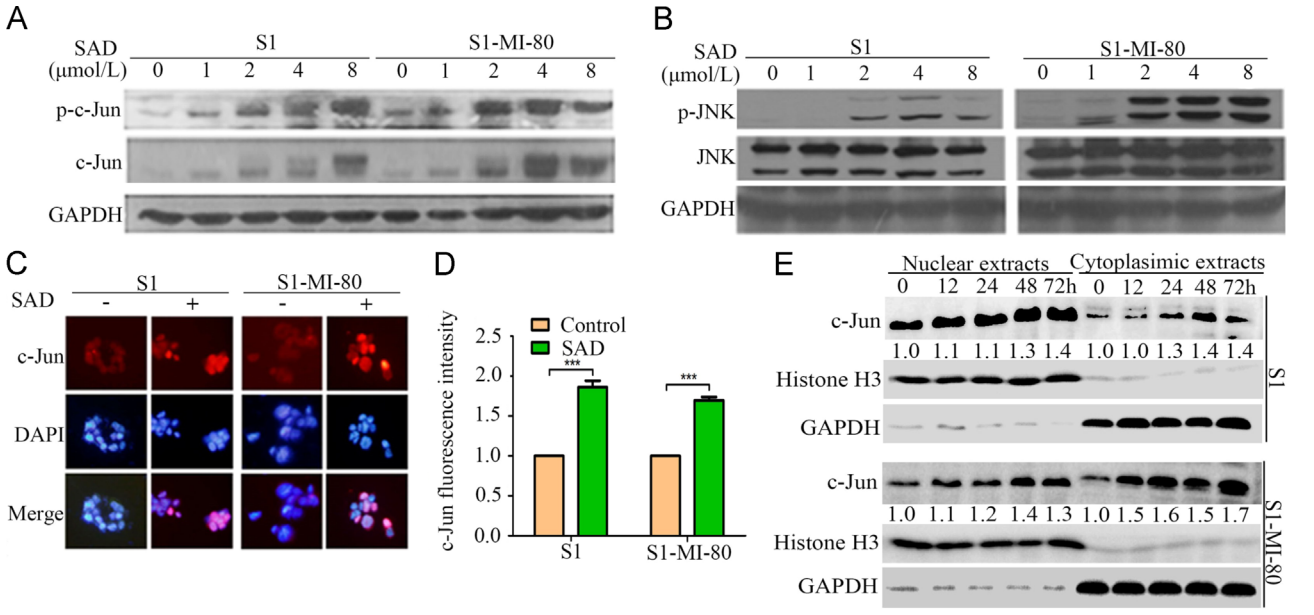

Figure 3 Effect of SAD on c-Jun expression and transportation. (A) After S1 and S1-MI-80 cells were treated with 0, 1, 2, 4, and 8 μmol/L SAD for 48 h, upregulation of c-Jun and p-c-Jun protein were observed. (B) After S1 and S1-MI-80 cells were treated with indicated concentrations of SAD for 48 h, JNK and phosphorylated JNK were up-regulated. (C) S1 and S1-MI-80 cells were treated with 4 μmol/L SAD for 48 h, respectively. c-Jun protein was measured by laser confocal microscopy as described in Methods. (D) Histograms of c-Jun fluorescence intensity in non-treated and treated S1 and S1-MI-80 cells. Each value represents the mean ± standard deviation of three independent experiments. $^{***}P < 0.001$, compared to the control group. (E) S1 and S1-MI-80 cells were treated with 4 μmol/L SAD for 12, 24, 48 and 72 h, respectively. Cytoplasmic and nuclear extract were separated on SDS-PAGE. c-Jun protein was detected by Western Blot assay as described in Methods. GAPDH and Histone H3 were used as a loading control to indicate cytoplasmic or nuclear protein respectively.

3.6. SAD stabilized c-Jun protein by decreasing proteasome-dependent degradation

As shown above, c-Jun protein was overexpressed in SAD-treated cells. Next, RT-PCR and qRT-PCR were used to detect the expression of c-Jun mRNA. However, these data showed that SAD did not up-regulate the mRNA level of c-Jun (Fig. 5A and B). To measure the effect of SAD on the stability of c-Jun protein, cycloheximide (CHX), an inhibitor of protein synthesis, was used to measure the half-life of c-Jun protein in cells treated with or without SAD. We found that SAD treatment completely attenuated the ability of CHX to decrease c-Jun expression, suggesting that the induction of c-Jun expression by SAD was due to inhibiting the degradation of c-Jun (Fig. 5C and D). To determine whether the SAD-mediated accumulation of c-Jun was generated *via* the proteasomal or lysosomal pathway, we used the proteasome inhibitor MG132 and the lysosomal inhibitor chloroquine combining with SAD in cells. Surprisingly, we found that both SAD and MG132 caused c-Jun and phosphor-c-Jun accumulation in the cells, but the same effect was not obtained with chloroquine (Fig. 5E). These results suggest that SAD enhances the protein level of c-Jun though inhibiting its degradation *via* proteasome pathway without interfering with its transcription.

3.7. c-Jun/Src/STAT3 played a key role in SAD-triggered apoptosis

The present results showed that SAD induced apoptosis in S1 and S1-MI-80 cells. Nevertheless, the underlying mechanism was not clear. We decided to analyze the potential mechanism involved in SAD-mediated apoptosis. As we described above, SAD activated JNK then subsequently phosphorylated and activated c-Jun which is a regulator of cell apoptosis. Abnormal activation of SRC and STAT3 is associated with the resistance of cancer cell apoptosis. Meanwhile, JNK signaling is correlated with the activity of SRC and STAT3.[18] In this study, we found that both the phosphorylated and total protein of SRC and STAT3 were decreased after SAD treatment (Fig. 6A). S1 and S1-MI-80 cells were transfected with a mock-vehicle and c-Jun plasmid to determine whether the SAD-induced inhibition of SRC and STAT3 was associated with an activation of c-Jun. The phosphorylated and total protein levels of SRC and STAT3 were both attenuated after the overexpression of c-Jun, these results were consistent with the efficacy of SAD treatment (Fig. 6B). Taken together, these results suggest that SAD induces MDR cells apoptosis through the c-Jun/SRC/STAT3 cascade.

4. Discussion

The researches on marine drugs initiated in the late 1970s[19]. Bioactive materials producing by marine organisms were demonstrated to have antitumor, anti-inflammatory, and antioxidant activities[20]. It is reported that marine-derived extracts and compounds can trigger the apoptotic death of cancer cells by inducing ROS generation[21]. In recent decades, a large number of marine compounds were found out to reverse MDR. Previous researches showed that SAD possessed anticancer properties, such as pro-apoptotic, anti-proliferative and anti-angiogenic effects[22], and downregulated the expression of ABCG2 to decrease the percentage of side population (SP) cells[6]. It was clarified that the

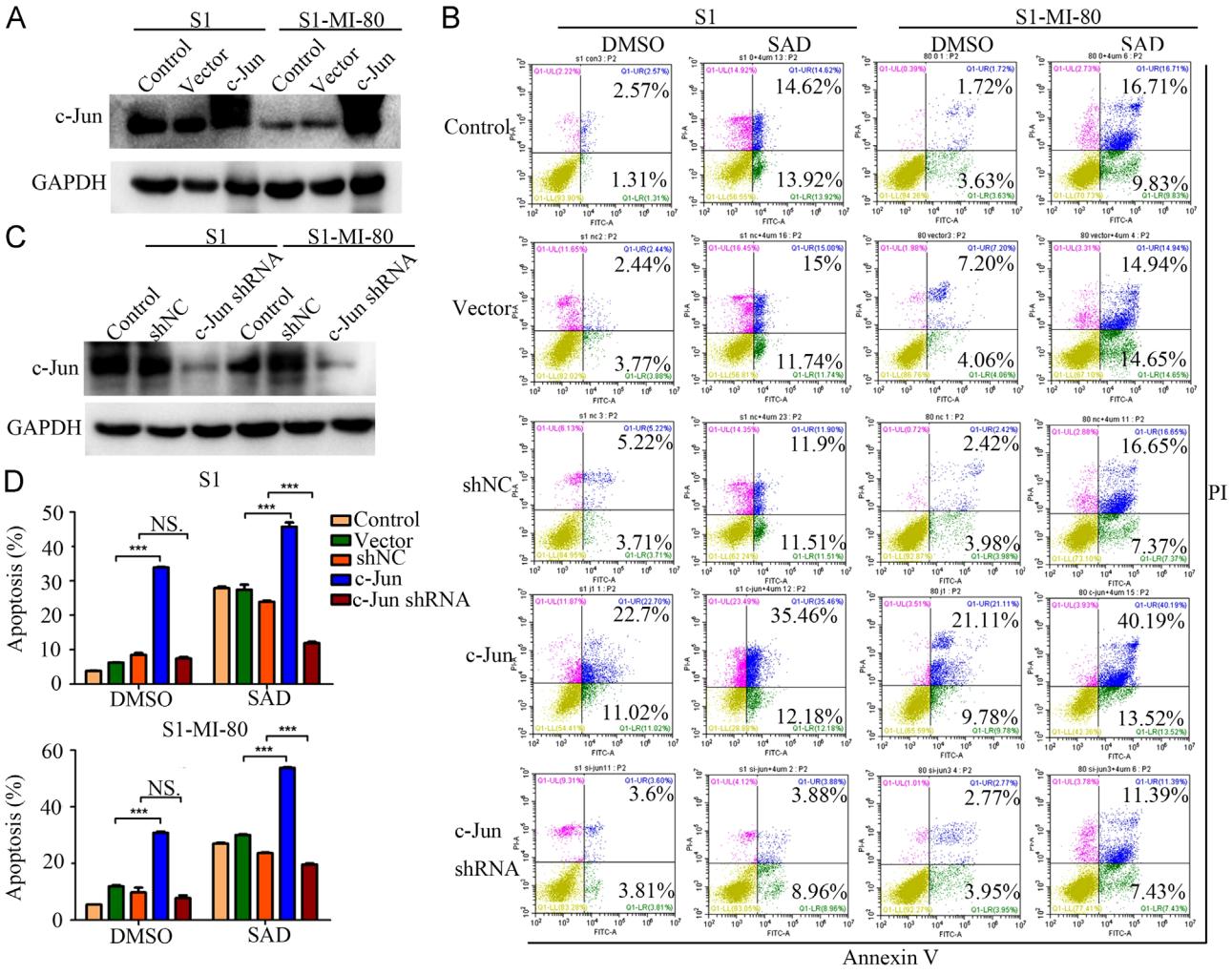

Figure 4 SAD stimulating cancer cells apoptosis by upregulation of c-Jun. (A) and (C) Western blot assay was used to detect c-Jun protein expression. (A) Transient transfection of c-Jun and pcDNA3.1 vector served as control was carried out in S1 and S1-MI-80 cells for 48 h. (C) Downregulation of c-Jun expression with stable transfection of their cognate shRNAs was confirmed with Western blot. (B) and (D) After 4 μmol/L SAD treatment, the apoptotic rate of cells was enhanced with c-Jun overexpression, while knockdown c-Jun with shRNA could attenuate SAD effects on programmed cell death.

mechanisms of MDR included the dysregulation of cell apoptosis, autophagy, the disorder of drug metabolism and drug targets[23]. To date, the mechanisms of the anticancer effect of SAD have not been fully studied. In this study, we showed that SAD reduced the proliferation of both MDR and their parental cancer cells and induced apoptosis by the activation of JNK/c-Jun signaling pathway and the subsequent inhibition of Src/STAT3 signaling.

Our prior research demonstrates that SAD induces leukemia cell apoptosis and cell cycle arrest through GSK-3*β*/*β*-catenin/c-Myc pathway[5]. In this study, we detected that SAD promoted G2/M phase arrest (Fig. 2A and B) and induced apoptosis in MDR cells (Fig. 2D and E). The G2/M phase arrest caused by SAD was due to the accumulation of phospho-CDC2 and the decrease of cyclin B1 (Fig. 2C). The cyclin B1/CDC2 complex is required for the progression of G2/M phase. The activation and dephosphorylation of CDC2 at Tyr15 is regulated by CDC25C, which is a critical regulator during G2/M transition[24]. SAD attenuated the expression of CDC2 and cyclin B1, and simultaneously it inactivated CDC2 through phosphorylating CDC2, resulting in the decreased formation of cyclin B1/CDC2 complex. We thought that these effects were associated with activating JNK signaling pathways which were related to G2/M phase arrest[25,26]. In this study, we showed that SAD executed cytotoxicity in three pairs of MDR and their parental sensitive cells. Therefore, SAD might be a novel agent for cancer treatment and even overcome drug resistance.

Previous studies revealed that the JNK signaling cascade was involved in the function of anticancer in ABCG2-overexpression MDR cells, and the activation of JNK signaling was accompanied by the phosphorylation of c-Jun[27,28]. As we know that JNK proteins form both homo- and heterodimers to influence the molecular functions of AP-1, including controlling cell cycle, proliferation, apoptosis, metastasis and even multidrug resistance. Herein, we suspected that SAD might be a promising antitumor compound *via* activation of JNK/c-Jun pathway. In this research, we discovered that SAD obviously increased the total and the phosphorylation level of JNK protein, as well as the phosphorylation level of c-Jun protein at serine-63 (Fig. 3A and B). These results are consistent with previous studies, which indicate that the phosphorylation at serine-63 in the NH_2-terminal transactivation domain of c-Jun by JNK is necessary to the activation of

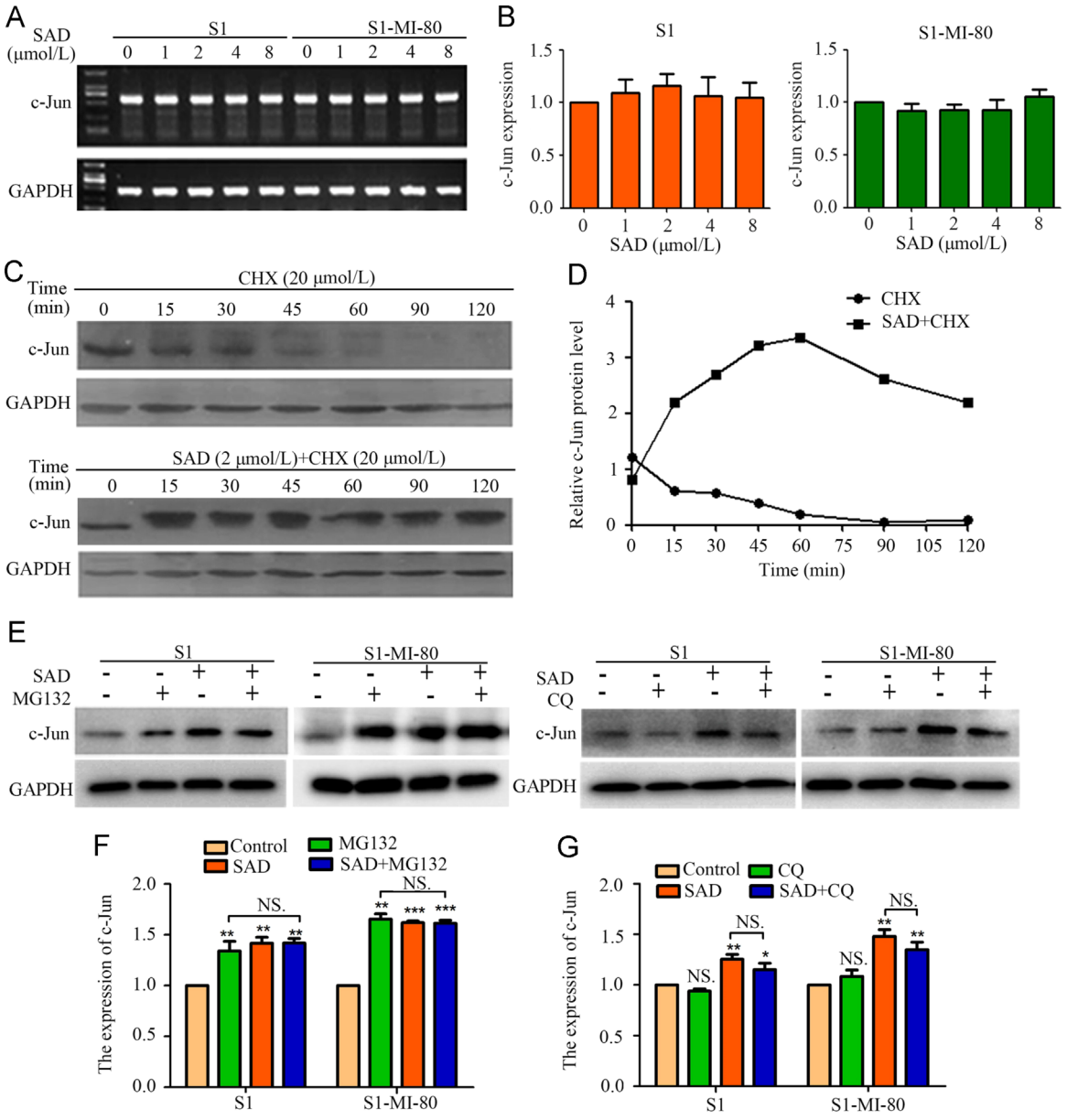

Figure 5 SAD regulated the expression of c-Jun protein in post-translation levels. (A) and (B) The mRNA levels of c-Jun were determined by RT-PCR and Real-time quantitative PCR. The expression of GAPDH was used as a loading control. (C) S1 cells were pre-incubated with 20 μg/mL CHX for 2 h. Then, S1 cells were treated with or without 4 μmol/L SAD. At different time points, cells were harvested and detected by Western blotting. (D) and (E) MG132 and chloroquine were used as the specific inhibitors for proteasome and lysosome, the expression of c-Jun and phosphor-c-Jun were detected after SAD treatment with or without MG132 (10 μmol/L) and chloroquine (50 μmol/L) at least 6 h, GAPDH was used as a loading control. (F) and (G) The graph demonstrates relative intensity of c-Jun compared to the untreated control and normalized against the loading control. $^{*}P < 0.05$, $^{**}P < 0.01$, $^{***}P < 0.001$, N.S (non-significant) *vs*. the control. Data were presented as mean ± SD from triplicate experiments.

endogenous c-Jun[29,30]. As a transcription factor, c-Jun has to transfer into the cell nucleus to conduct functions[15,17]. We confirmed that SAD activated c-Jun and promoted its translation from cytoplasm to nucleus in S1 and S1-MI-80 cells (Fig. 3C, D and E). Furthermore, we showed that SAD increased the protein level of c-Jun with its mRNA expression unchanged (Fig. 5A–C). It was reported that the phosphorylation of c-Jun by JNK not only resisted multi-ubiquitination but also stabilized c-Jun protein, and consequently caused the accumulation of c-Jun protein[31]. It was reported that c-Jun formed a complex with activated C-kinase 1 (Rack1) and ubiquitin ligase Fbw7, then c-Jun could be released from the complex and escaped from degradation by proteasome system[32,33]. In this study, we also found that c-Jun was upregulated by the inhibition of the proteasome pathway but not lysosomal pathway (Fig. 5D and E). Further studies are needed to reveal the molecular mechanism of the degradation of c-Jun *via* proteasome way after SAD treatment.

Notably, c-Jun is responsible to the programmed cell death of cancer cells. We propose that SAD might regulate apoptosis through stimulating c-Jun expression. We observed that

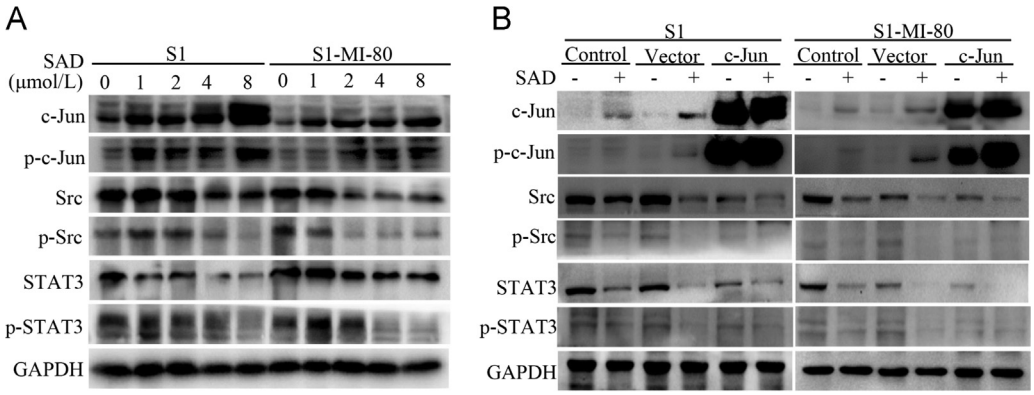

Figure 6 SAD regulated apoptosis through c-Jun/SRC/STAT3. (A) Western blot showed the protein levels of SRC and STAT3 in SAD mediated S1 and S1-MI-80 cells. (B) Overexpression of c-Jun decreased SRC and STAT3 expression as the similar effect of SAD. GAPDH was used as loading control.

the upregulation of c-Jun enhanced apoptosis in MDR cells, and the stable knockdown of c-Jun reversed these effects of SAD (Fig. 4B and D). Next, we continued to investigate the mechanism of SAD-induced apoptosis. SRC/STAT3 activation potentiates both proliferative and anti-apoptotic signaling and even is associated with chemoresistance[34]. In our study, we found that not only the total protein and phosphorylation levels of c-Jun but also SRC and STAT3 were changed following SAD exposure, which suggested that c-Jun is related with both Src and STAT3 (Fig. 6A). It was consistent with the finding that JNK signaling could not induce the activation of STAT3 in the absence of SRC[35]. Meanwhile, Marco and his colleagues[36] demonstrated that suppressing JAK/STAT led to the non-autonomous expansion of JNK, which could promote excessive cell apoptosis and tissue damage. We used overexpression plasmid of c-Jun to transfect colon cancer cells, the total and phosphorylation protein levels of SRC and STAT3 were found to be weakened (Fig. 6B). Hence, our results supported that the downregulation of SRC and STAT3 were caused by c-Jun activity, but whether the reduced expression of STAT3 may cause further elevation of c-Jun needs to be further study. However, the specific mechanism of how c-Jun regulates SRC/STAT3 signaling to promote S1 and S1-MI-80 cells apoptosis needs further investigation. In addition, some reports provided informative evidence for the cellular apoptosis induced by c-Jun. For instance, the upregulation of c-Jun promoted the transcription of *FasL* which subsequently caused Fas/FasL-mediated apoptosis[37]; the activation of c-Jun contributed to the intrinsic proapoptotic mechanism by upregulating apoptosis-related proteins, such as BIM[38] and caspase-3[39].

In summary, we provided insight into the possible mechanisms of the SAD-induced G2/M phase arrest in MDR and their parental sensitive cells. Our results further indicate that c-Jun facilitates apoptosis through inhibiting JNK/c-Jun/SRC/STAT3 signaling. Meanwhile, the protein level of c-Jun was elevated by resisting from the proteasomal-mediated degradation after SAD treatment. These findings suggest that SAD which functions as a positive regulator of c-Jun may be a potential compound of acquiring therapeutic effects in MDR cells and deserve further study in the future.

Acknowledgments

The authors thank Dr. Susan Bates (NCI, NIH, Bethesda, MD, USA) for the ABCG2-overexpressing cell lines. This work was supported by grants from the National Science & Technology Major Project "Key New Drug Creation and Manufacturing Program" (No. 2018ZX09711002, China), Science and Technology Foundation of Guangdong Province (No. 2016A030312014, China), Guangzhou Science and Technology Program (No. 201707010048, China) and from the Scientific and Technological Leading Talent Project of Guangdong Province (2015, China).

Availability of data and materials

The authenticity of this article was validated by uploading the key data onto the Research Data Deposit public platform (www.researchdata.org.cn), and the approval RDD number is RDDB2018000421.

References

1. Simmons TL, Andrianasolo E, McPhail K, Flatt P, Gerwick WH. Marine natural products as anticancer drugs. *Mol Cancer Ther* 2005;**4**:333–42.
2. Glaser KB, Mayer AM. A renaissance in marine pharmacology: from preclinical curiosity to clinical reality. *Biochem Pharmacol* 2009;**78**:440–8.
3. Bian J, Song F, Zhang L. Strategies on the construction of high-quality microbial natural product library—a review. *Acta Microbiol Sin* 2008;**48**:1132–7.
4. Guo Z, She Z, Shao C, Wen L, Liu F, Zheng Z, et al. ^{1}H and ^{13}C NMR signal assignments of paecilin A and B, two new chromone derivatives from mangrove endophytic fungus Paecilomyces sp. (tree 1–7). *Magn Reson Chem* 2007;**45**:777–80.
5. Zhang JY, Tao LY, Liang YJ, Yan YY, Dai CL, Xia XK, et al. Secalonic acid D induced leukemia cell apoptosis and cell cycle arrest of G_1 with involvement of GSK-3β/β-catenin/c-Myc pathway. *Cell Cycle* 2009;**8**:2444–50.
6. Hu YP, Tao LY, Wang F, Zhang JY, Liang YJ, Fu LW. Secalonic acid D reduced the percentage of side populations by down-regulating the expression of ABCG2. *Biochem Pharmacol* 2013;**85**:1619–25.
7. Qi XM, Wang F, Mortensen M, Wertz R, Chen G. Targeting an oncogenic kinase/phosphatase signaling network for cancer therapy. *Acta Pharm Sin B* 2018;**8**:511–7.
8. Sui H, Zhou S, Wang Y, Liu X, Zhou L, Yin P, et al. COX-2 contributes to P-glycoprotein-mediated multidrug resistance *via* phosphorylation of c-Jun at Ser63/73 in colorectal cancer. *Carcinogenesis* 2011;**32**:667–75.
9. Tomiyasu H, Watanabe M, Sugita K, Goto-Koshino Y, Fujino Y, Ohno K, et al. Regulations of ABCB1 and ABCG2 expression through MAPK pathways in acute lymphoblastic leukemia cell lines. *Anticancer Res* 2013;**33**:5317–23.

10. Bohmann D, Bos TJ, Admon A, Nishimura T, Vogt PK, Tjian R. Human proto-oncogene c-jun encodes a DNA binding protein with structural and functional properties of transcription factor AP-1. *Science* 1987;**238**:1386–92.
11. Karin M, Hawkins PT, Irvine RF, Michell RH, Marshall CJ. The regulation of AP-1 activity by mitogen-activated protein kinases. *Philos Trans Roy Soc Lond Ser B Biol Sci* 1996;**351**:127–34.
12. Kollmann K, Heller G, Sexl V. c-JUN prevents methylation of $p16^{INK4a}$ (and *Cdk6*): the villain turned bodyguard. *Oncotarget* 2011;**2**:422–7.
13. Ishdorj G, Johnston JB, Gibson SB. Cucurbitacin-I (JSI-124) activates the JNK/c-Jun signaling pathway independent of apoptosis and cell cycle arrest in B leukemic cells. *BMC Cancer* 2011;**11**:268.
14. Tao LY, Liang YJ, Wang F, Chen LM, Yan YY, Dai CL, et al. Cediranib (recentin, AZD2171) reverses ABCB1- and ABCC1-mediated multidrug resistance by inhibition of their transport function. *Cancer Chemother Pharmacol* 2009;**64**:961–9.
15. Dhulipala VC, Welshons WV, Reddy CS. Inhibition of human embryonic palatal mesenchymal cell cycle by secalonic acid D: a probable mechanism of its cleft palate induction. *Orthod Craniofac Res* 2004;**7**:227–36.
16. Sui H, Cai GX, Pan SF, Deng WL, Wang YW, Chen ZS, et al. miR200c attenuates P-gp-mediated MDR and metastasis by targeting JNK2/c-Jun signaling pathway in colorectal cancer. *Mol Cancer Ther* 2014;**13**:3137–51.
17. Eferl R, Wagner EF. AP-1: a double-edged sword in tumorigenesis. *Nat Rev Cancer* 2003;**3**:859–68.
18. Chatterjee M, Ben-Josef E, Thomas DG, Morgan MA, Zalupski MM, Khan G, et al. Caveolin-1 is associated with tumor progression and confers a multi-modality resistance phenotype in pancreatic cancer. *Sci Rep* 2015;**5**:10867.
19. Fenical W. New pharmaceuticals from marine organisms. *Trends Biotechnol* 1997;**15**:339–41.
20. Hu X, Zhang Z, Liu T, Song L, Zhu J, Guo Z, et al. Polypeptide Fraction from *Arca subcrenata* induces apoptosis and G2/M phase arrest in Hela cells *via* ROS-mediated MAPKs pathways. *Evid Based Complement Altern Med* 2015;**2015**:930249.
21. Farooqi AA, Fayyaz S, Hou MF, Li KT, Tang JY, Chang HW. Reactive oxygen species and autophagy modulation in non-marine drugs and marine drugs. *Mar Drugs* 2014;**12**:5408–24.
22. Guru SK, Pathania AS, Kumar S, Ramesh D, Kumar M, Rana S, et al. Secalonic acid-D represses HIF1α/VEGF-mediated angiogenesis by regulating the Akt/mTOR/p70S6K signaling cascade. *Cancer Res* 2015;**75**:2886–96.
23. An X, Sarmiento C, Tan T, Zhu H. Regulation of multidrug resistance by microRNAs in anti-cancer therapy. *Acta Pharm Sin B* 2017;**7**:38–51.
24. Cho YC, Park JE, Park BC, Kim JH, Jeong DG, Park SG, et al. Cell cycle-dependent Cdc25C phosphatase determines cell survival by regulating apoptosis signal-regulating kinase 1. *Cell Death Differ* 2015;**22**:1605–17.
25. Liao YJ, Bai HY, Li ZH, Zou J, Chen JW, Zheng F, et al. Longikaurin A, a natural ent-kaurane, induces G2/M phase arrest *via* downregulation of SKP2 and apoptosis induction through ROS/JNK/c-Jun pathway in hepatocellular carcinoma cells. *Cell Death Dis* 2014;**5**:e1137.
26. Zhang J, Zhu X, Li H, Li B, Sun L, Xie T, et al. Piperine inhibits proliferation of human osteosarcoma cells *via* G2/M phase arrest and metastasis by suppressing MMP-2/-9 expression. *Int Immunopharmacol* 2015;**24**:50–8.
27. Alam SK, Yadav VK, Bajaj S, Datta A, Dutta SK, Bhattacharyya M, et al. DNA damage-induced ephrin-B2 reverse signaling promotes chemoresistance and drives EMT in colorectal carcinoma harboring mutant p53. *Cell Death Differ* 2016;**23**:707–22.
28. Zhu MM, Tong JL, Xu Q, Nie F, Xu XT, Xiao SD, et al. Increased JNK1 signaling pathway is responsible for ABCG2-mediated multidrug resistance in human colon cancer. *PLoS One* 2012;**7**:e41763.
29. Huang CH, Chen YJ, Chao TY, Liu WH, Changchien JJ, Hu WP, et al. The association between p38 MAPK-mediated TNF-α/TNFR2 up-regulation and 2-(4-aminophenyl)-7-methoxybenzothiazole-induced apoptosis in human leukemia U937 cells. *J Cell Physiol* 2016;**231**:130–41.
30. Whang YM, Jin SB, Park SI, Chang IH. MEK inhibition enhances efficacy of bacillus Calmette-Guérin on bladder cancer cells by reducing release of Toll-like receptor 2-activated antimicrobial peptides. *Oncotarget* 2017;**8**:53168–79.
31. Musti AM, Treier M, Bohmann D. Reduced ubiquitin-dependent degradation of c-Jun after phosphorylation by MAP kinases. *Science* 1997;**275**:400–2.
32. Zhang J, Zhu F, Li X, Dong Z, Xu Y, Peng C, et al. Rack1 protects N-terminal phosphorylated c-Jun from Fbw7-mediated degradation. *Oncogene* 2012;**31**:1835–44.
33. Marsolier J, Perichon M, DeBarry JD, Villoutreix BO, Chluba J, Lopez T, et al. *Theileria* parasites secrete a prolyl isomerase to maintain host leukocyte transformation. *Nature* 2015;**520**:378–82.
34. Kim JH, Lee Y, Kim MY, Cho JY. 4-(*Tert*-butyl)-2,6-bis(1-phenylethyl)phenol induces pro-apoptotic activity. *Korean J Physiol Pharmacol* 2016;**20**:253–9.
35. Turkson J, Bowman T, Adnane J, Zhang Y, Djeu JY, Sekharam M, et al. Requirement for Ras/Rac1-mediated p38 and c-Jun N-terminal kinase signaling in Stat3 transcriptional activity induced by the Src oncoprotein. *Mol Cell Biol* 1999;**19**:7519–28.
36. La Fortezza M, Schenk M, Cosolo A, Kolybaba A, Grass I, Classen AK. JAK/STAT signalling mediates cell survival in response to tissue stress. *Development* 2016;**143**:2907–19.
37. Wang SW, Chen YR, Chow JM, Chien MH, Yang SF, Wen YC, et al. Stimulation of Fas/FasL-mediated apoptosis by luteolin through enhancement of histone H3 acetylation and c-Jun activation in HL-60 leukemia cells. *Mol Carcinog* 2018;**57**:866–77.
38. Tomicic MT, Meise R, Aasland D, Berte N, Kitzinger R, Krämer OH, et al. Apoptosis induced by temozolomide and nimustine in glioblastoma cells is supported by JNK/c-Jun-mediated induction of the BH3-only protein BIM. *Oncotarget* 2015;**6**:33755–68.
39. Song B, Xie B, Wang C, Li M. Caspase-3 is a target gene of c-Jun: ATF2 heterodimers during apoptosis induced by activity deprivation in cerebellar granule neurons. *Neurosci Lett* 2011;**505**:76–81.